

Research article

A novel approach in control release monitoring of protein-based bioactive substances from injectable PLGA-PEG-PLGA hydrogel

Klára Lysáková^{1*}, Kristýna Hlináková¹, Kateřina Kutálková², Radka Chaloupková²,
Jan Židek¹, Jana Brtníková¹, Lucy Vojtová¹

¹Brno University of Technology, CEITEC-Central European Institute of Technology, Purkyňova 656/123, 612 00 Brno, Czech Republic

²Enantis Ltd., Kamenice 771/34, 625 00 Brno, Czech Republic

Received 31 January 2022; accepted in revised form 5 April 2022

Abstract. In recent times, autologous fat grafting has emerged as one of the most popular techniques for restoring volume depletion. Although the retention predictability of grafted fat has been improved, the quality of grafted tissue is still unsatisfactory. Unpredictable volume loss and low-fat survival is a major problem after application. Biodegradable PLGA-PEG-PLGA (poly(lactic-co-glycolic acid)-*b*-poly(ethylene glycol)-*b*-poly(lactic-co-glycolic acid)) hydrogel delivery system enriched with stable fibroblast growth factor 2 (FGF2-STAB[®]), due to its properties, seems to be attractive material that will help to increase fat life. In this study, the mechanism of FGF2-STAB[®] release from an injectable thermosensitive and biodegradable PLGA-PEG-PLGA hydrogel was monitored. First-order kinetics were controlled mainly by decreasing the concentration of an active compound in the matrix and, at a later stage, by matrix degradation. Furthermore, the activity of the protein after release from the hydrogel matrix was studied. No loss of FGF2-STAB[®] activity in the dynamic system after 14 days has been detected. The development of such a drug delivery system appears promising for further use in reconstructive medicine *e.g.*, in mixing with fat graft being the subject of current research.

Keywords: biodegradable polymers, drug delivery system, thermosensitive hydrogel, PLGA-PEG-PLGA copolymer, FGF2-STAB[®]

1. Introduction

In the last decade, lipografting or fat transfer has found its place in reconstructive and plastic surgery [1, 2], as surgical procedures significantly contribute to improving functional and aesthetic outcomes after severe soft tissue trauma and scar contracture [3, 4]. These injuries often lead to long-term consequences, further treatment, or even disability. The biggest disadvantage of lipografting is the unpredictable volume loss after application requiring the initial over-correction and multiple operations to provide appropriate volume and contours [5]. Biodegradable

hydrogels suitable for the drug carrier are a possible solution in combination with lipoaspirate to solve the problem of increasing the percentage survival of the fat graft. Another advantage of ‘smart’ injectable temperature-responsive hydrogels is a simple application to areas that are difficult to access or inaccessible in surgery and form gel at human body temperature [6]. This drug delivery system has significant advantages over traditional drug forms. Benefits include topical drug delivery, reduced dosage frequency, diminished *in vivo* fluctuation of drug concentration and maintenance of

*Corresponding author, e-mail: klara.lysakova@ceitec.vutbr.cz
© BME-PT

drug concentration in the desired range, and evaluation of side effects [7].

A thermosensitive poly(lactic-*co*-glycolic acid)-*b*-poly(ethylene glycol)-*b*-poly(lactic-*co*-glycolic acid) (PLGA-PEG-PLGA) copolymer, where the individual segments (PLGA and PEG copolymers) are approved by the Food and Drug Administration (FDA), is suitable material for this application [8–13]. Nowadays, drug scaffolds based on PLGA-PEG-PLGA copolymers are already commercially available under the names ReGel® and OncoGel®, releasing under a controlled manner either the hydrophilic hormone insulin (for diabetes treatment) or the hydrophobic drug paclitaxel (for cancer treatment), respectively [14–16]. PLGA-PEG-PLGA consists of two hydrophobic segments (PLGA) and one hydrophilic segment (PEG) placed in the middle. Thanks to the amphiphilic properties, the copolymer self-assembles and physically cross-links into flower-shaped micelles above the critical micellar concentration (CMC), creating an elastic gel in an aqueous environment [18–21]. The gelation temperature of the copolymer solution and the degradation rate of the formed gel depends on the ratios between the copolymer components. The rate of hydrogel degradation depends on the D,L-lactide (LA)/glycolide (GA) molar ratio. The degradation rate is slower with a higher LA/GA ratio. Hydrophobic interaction among copolymer blocks is stronger because of the higher content of hydrophobic LA molecules. The gelation temperature is based on the same principle. Increasing the LA/GA ratio leads to a decrease in the sol-gel transition [22–24].

Another acceleration of postoperative treatment is the addition of bioactive agents to the hydrogel carrier [25]. The protein-based drug used in this work belongs to the group of fibroblast growth factors that promote healing and lead to tissue remodeling. Fibroblast growth factor 2 (FGF2) stimulates the growth and formation of new vessels (angiogenesis), leading to better wound healing and tissue development and contributing to the pathogenesis of various diseases (cancer or atherosclerosis) [26]. Thermostable variant of FGF2, FGF2-STAB® exhibits higher resistance toward elevated temperature and extended half-life at 37 °C for up to 20 days [27, 28]. FGF2-STAB® has been used in several *in vitro* and *in vivo* studies of our group under a broad multidisciplinary collaboration to accelerate and enhance tissue healing (Muchová et al. [29], Vojtová et al. [30], Krtička et

al. [31]). In this research, the release of bioactive proteins from the hydrogel scaffold and further its biological activity was studied as an essential parameter for the potential application in reconstructive surgery to support the effectiveness of lipografting procedure.

2. Experimental section

2.1. Synthesis and purification of

PLGA-PEG-PLGA copolymer

A thermosensitive biodegradable poly(lactic-*co*-glycolic acid)-*b*-poly(ethyleneglycol)-*b*-poly(lactic-*co*-glycolic acid) PLGA-PEG-PLGA hydrogel was used as a carrier for the treatment-promoting protein. The triblock copolymer (ABA type) with a D, L-LA/GA molar ratio of 3.0 and a PLGA/PEG weight ratio of 2.5 (D,L-LA ≥99.5% and GA ≥99.9% – Polysciences, USA, PEG M_w 1500 g·mol⁻¹ – Merck, Germany) was synthesized by ring-opening polymerization (ROP) under a nitrogen atmosphere. The reaction was carried out using a tin catalyst (Sn(II) 2-ethylhexanoate ≥92.5% – Merck, USA) at 130 °C for 3 hours. The final copolymer was purified from the unreacted monomer by dissolving in ultrapure water and then heating to 80 °C. The precipitated copolymer was separated by decantation. The purification process was repeated three times, followed by the freeze-drying of the final product [32].

2.2. PLGA-PEG-PLGA hydrogel preparation

The polymer was dissolved according to the required concentration in phosphate buffer – PBS (20 mM PBS, 150 mM NaCl, pH 7.5) at magnetic stirrer for 3 days at 12 °C.

Characterization of PLGA-PEG-PLGA Copolymer

The copolymer was characterized using gel permeation chromatography (GPC) and nuclear magnetic resonance (NMR). Dynamic rheological analysis was used to determine the course of hydrogel gelation. Gel permeation chromatography (GPC)/size exclusion chromatography (SEC) with multi-angle light scattering detector (MALS, DAWN HELIOS-II, Wyatt, USA) and refractometer (T-rEX, Wyatt, USA) was used to determine the number of average molecular weight (\bar{M}_n) and the polydispersity index (M_w/M_n). Two PLgel 5 µm Mixed-C columns were used for separation, and tetrahydrofuran (THF for high performance liquid chromatography – HPLC, ≥99.9% – Merck, USA) with a flow rate of 1 ml·min⁻¹ was used as the mobile phase. An analytical standard

for GPC/SEC polystyrene (PS) with a molecular weight of $M_w = 30\,000\text{ g}\cdot\text{mol}^{-1}$ and $PDI = M_w/M_n = 1.06$ was used to calibrate the system; however, the data obtained were absolute due to the setup of the detectors. For measurement, $15\text{ mg}\cdot\text{mL}^{-1}$ PLGA-PEG-PLGA copolymer dissolved in tetrahydrofuran (THF) was dosed. All measured data were evaluated using Astra software.

The results of the molecular weight and polymer characterization were confirmed using proton nuclear magnetic resonance ^1H NMR spectroscopy on a 500 MHz NMR spectrometer (Bruker, Germany) Advance NEO instrument using 128 scans in deuterated chloroform solvent (CDCl_3 – Merck, USA) solvent at 25°C . Chemical shifts in ppm were reported in relation to tetramethyl silane (TMS – Merck, USA). ^1H NMR spectra were evaluated using an ACD/ ^1D NMR Processor.

The rheological analysis was performed using a stress-controlled rotation rheometer (AR-G2, TA Instruments, USA). The 15 wt% PLGA-PEG-PLGA solution in PBS (20 mM PBS, 150 mM NaCl, pH 7.5) was used to characterize the storage and the loss moduli, thereby determining the start of gelation of the copolymer solution together with the decay temperature of the gel. To measure the temperature dependence, a cone-plate geometry with a diameter of 40 mm and 2° angle was used. The hydrogel solution was injected into Peltier by syringe, and the working position (geometric gap of $60\text{ }\mu\text{m}$) was established. A water-filled solvent trap was used to prevent solvent evaporation during the experiment. The temperature ramp was set between 20 – 50°C with a heating rate of 0.5°C per minute. All measurements were performed at a constant frequency of $1\text{ rad}\cdot\text{s}^{-1}$ and 0.4 Pa [15].

2.3. Degradation of the PLGA-PEG-PLGA hydrogel

Weight loss and pH change of the 15 wt% hydrogel was measured over time. The dissolved samples, according to the sample preparation chapter, were moved into inserts (SPLInsert™ Hanging, 6 Inserts/6 well plate, PC, $0.4\text{ }\mu\text{m}$, Thermo Fisher Scientific, USA), to the bottom pan, PBS solvent was added, and the samples were left in the incubator at 37°C . The hydrogel degraded through the membrane ($0.4\text{ }\mu\text{m}$) into a solvent. At certain time intervals, the solution was removed from the bottom pan. The insert with the hydrogel was weighed to determine

weight loss, followed by refilling the bottom pan with the same volume of fresh solution, and the insert was put back to continue the degradation process monitoring. Furthermore, the pH (Verkon, Czech Republic) of the hydrogel alone was measured.

2.4. Protein-enriched PLGA-PEG-PLGA hydrogels preparation

Hydrogels, according to chapter sample preparation, were prepared so that the final concentration of gels after the addition of the bioactive substance albumin human (Merck, USA), lysozyme human, (Merck, USA) and FGF2-STAB® (Enantis Ltd., Czech Republic [28]) were 15 wt%. Protein or enzyme concentration in each scaffold was $100\text{ }\mu\text{g}\cdot\text{mL}^{-1}$ the whole mixture was stirred at 12°C for 30 minutes and at room temperature for 15 minutes. Subsequently, the sample was transferred to the cultivation plate inserts (SPL Insert™ Hanging, 6 Inserts/6 well plate, PC, $0.4\text{ }\mu\text{m}$, Thermo Fisher Scientific, USA). Inserts proved to be appropriate when proteins or enzymes were released into the PBS-filled trays through the membrane while the degraded polymer could not go through (see Figure 1).

The release mechanism of bioactive substances was measured by two methods, namely UV-VIS spectrophotometry in the presence of Bradford reagent and SDS-PAGE electrophoresis. The measurement procedures are as follows.

2.4.1. UV-VIS spectrophotometry with Bradford reagent

The UV-VIS spectrophotometer (Jasco V-730, Japan, Biochrom Libra S22, UK) was used to measure the amount of proteins released from the thermosensitive PLGA-PEG-PLGA hydrogel. The measurement was carried out at a constant wavelength of 595 nm. A Bradford reagent (for 0.1 – $1.4\text{ mg}\cdot\text{mL}^{-1}$ protein – Merck, USA) that interacts with proteins was used to shift the maximum absorption from 280 to 595 nm. Three calibration curves were created for the protein measurement in a concentration range of 1–10, 10–100 and 50 – $750\text{ mg}\cdot\text{mL}^{-1}$. The pipetting ratios of the Bradford and sample quantities are shown in Table 1.

2.4.2. SDS-PAGE electrophoresis

Sodium dodecylsulphate-poly(acrylamide) electrophoresis (SDS-PAGE electrophoresis by VWR, USA) was used to determine the amount of FGF2-STAB®

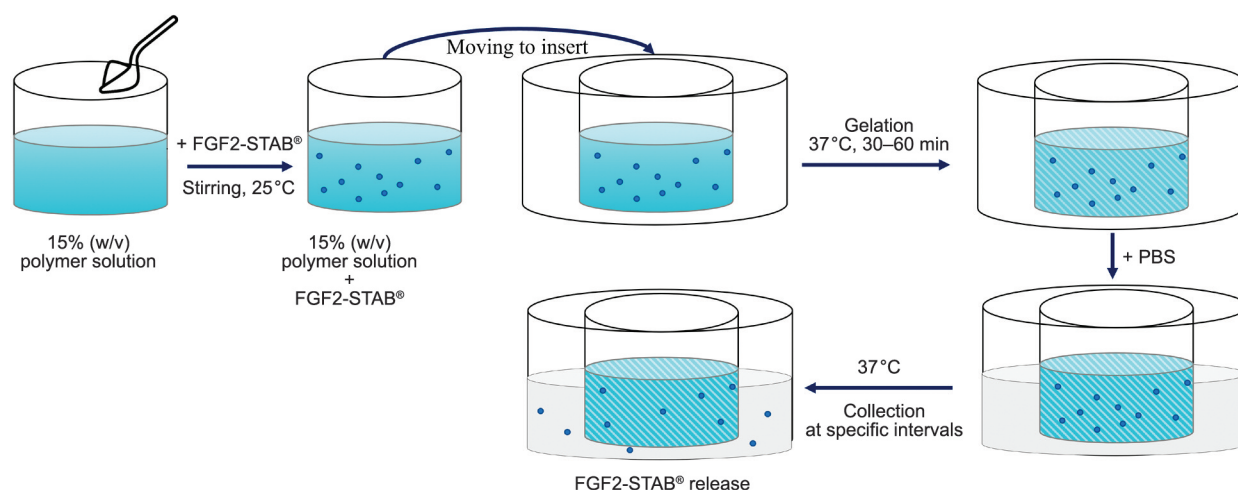


Figure 1. Sample preparation scheme for measurement – 15 wt% PLGA-PEG-PLGA solution + FGF2-STAB®.

Table 1. Reagent/sample pipetted volume for different concentrations.

	Bradford agent [μl]	Sample [μl]
Low concentration (1–10 mg·ml ⁻¹)	500	500
Middle concentration (10–100 mg·ml ⁻¹)	800	200
High concentration (50–750 mg·ml ⁻¹)	1000	30

released from the hydrogel matrix. The sodium dodecylsulphate (SDS) binds non-covalently to proteins, giving them a uniform negative charge, thus ensuring separation based solely on protein size [33]. The sample was pipetted into the Eppendorf tube, SDS dye (Sodium dodecyl sulphate ≥98.5% – Merck, USA, Mercaptoethanol 99% – Merck, USA and Coomassie Brilliant Blue R-250 – BIO-RAD, USA) was added. The entire solution was mixed and heated at 95 °C for 5 min. From 15% resolving gel (Resolving buffer 1.5M Tris-HCl pH 8.8, Acrylamide 30% – Merck, USA, MilliQ, Ammonium persulfate – APS ≥98% – Merck, USA, Sodium dodecyl sulphate – SDS ≥98.5% – Merck, USA, *N,N,N',N'*-Tetramethylethylenediamine – TEMED – Merck, USA) and 5% stacking gel (Stacking buffer 0.5M Tris-HCl pH 6.8, Acrylamide 30% – Merck, USA, MilliQ, APS ≥98% – Merck, USA, SDS ≥98.5% – Merck, USA, TEMED – Merck, USA) were prepared gel and 20 μl of the sample was added to the gel. The voltage was set to 120 V, the current to 400 mA, and the time to 200 min.

2.5. Protein biological activity measurement

The biological activity of FGF2-STAB® was tested using the BaF3 model system. BaF3 cells are

interleukin-3 (IL-3) dependent and naturally do not express any FGF receptors. Stable transgenic cell lines with all major FGF receptors are available [34]. In the absence of IL-3, these transgenic BaF3 cells rely solely upon FGFs for their proliferation. The most relevant receptor for FGF2 is FGFR2c, therefore the BaF3-FGFR2c cell line was used.

BaF3 cells expressing FGFR2c receptor [32] were cultured in full medium (RPMI 1640 medium with stable Glutamine – BioSera, China, 10% newborn calf serum – Sigma-Aldrich, USA, 1% PenicillinG/Streptomycin Sulfate – Gibco, USA, 50 μM β-mercaptoethanol – Gibco, USA, 600 μg·ml⁻¹ G418 disulfate salt – Sigma-Aldrich, USA, 0.5 ng·ml⁻¹ mouse interleukin 3 (IL-3) – Peprotech, UK) at 37 °C, 5% CO₂ (carbon dioxide) and passaged twice a week with 1:4 split ratio. Prior to the experiment, cells were collected and washed three times to remove any trace of IL-3.

For BaF3 proliferation assays, 40·10³ cells per well were seeded 96-well plates in 150 μl of assay medium (RPMI 1640 medium with stable Glutamine – BioSera, China, 10% newborn calf serum – Sigma-Aldrich, USA, 1% PenicillinG/Streptomycin Sulfate – Gibco, USA, 50 μM β-mercaptoethanol – Gibco, USA, 2 μg·ml⁻¹ heparin – Sigma-Aldrich, USA) and incubated for 24 hours at 37 °C, 5% CO₂. After 24 hours of starvation, 50 μl of tested samples of different concentrations were added to their respective test plates. The FGF2-STAB® content in each sample was determined earlier, and for the biological activity testing, a stock solution of 2 μg·ml⁻¹ and further serial dilutions were prepared. Medium with IL-3 was used as a positive control and plain assay medium as a negative control.

48 hours after FGF2-STAB® treatment, 20 μl of re-sazurin solution ($0.1 \text{ mg}\cdot\text{ml}^{-1}$, Sigma-Aldrich, USA) was added to each well. The extent of cell proliferation was measured by fluorescence detection of the final product after 12–15 hours of incubation at 37°C , 5% CO_2 .

3. Results

3.1. PLGA-PEG-PLGA polymer characterization (GPC, ^1H NMR)

Since we cannot obtain one molecular weight number for polymers, we determine its average value. The number average molecular weight (M_n) was verified by gel permeation chromatography (GPC) or size exclusion chromatography (SEC) for all batches (number of replicates, n . 10). Table 2 shows the mean of the number of average molecular weights. Figure 2 shows the determined molecular weight distribution of the polymer (curve 1) and Mark-Houwink plot (curve 2), providing information about the polymer linearity.

PLGA/PEG ratio and LA/GA (n . 1) ratio were determined by proton nuclear magnetic resonance spectroscopy (^1H NMR). The characteristic spectrum of the PLGA-PEG-PLGA copolymer with six clear peaks shows Figure 3. Deuterated chloroform was used as the solvent and corresponded to the peak with the largest shift. The lactic acid proton ($\text{O}-(\text{CH}_3)\text{CHO}$) is with the lowest chemical shift $\delta = 1.4\text{--}1.65 \text{ ppm}$ (e). ($\text{O}-(\text{CH}_3)\text{CHO}$) (a) corresponds to the $\delta = 5.1\text{--}5.3 \text{ ppm}$, and the peak with the shift in the area $\delta = 3.5\text{--}3.7 \text{ ppm}$ stands for the polyethylene glycol proton ($\text{OCH}_2\text{CH}_2\text{O}$) (d). By shifting in the area $\delta = 4.6\text{--}4.9 \text{ ppm}$, the glycolic acid proton (OCH_2O) (b) is observed. The peak with the lowest intensity $\delta = 4.2\text{--}4.35 \text{ ppm}$ corresponds to the proton from the $-\text{CH}_2-$ group in the bond between PEG and PLA ($\text{OCH}_2\text{CH}_2\text{O}$) (c). [35]. The number average molecular weight, the PLGA/PEG weight ratio, and the LA/GA molar ratio are shown in Table 2.

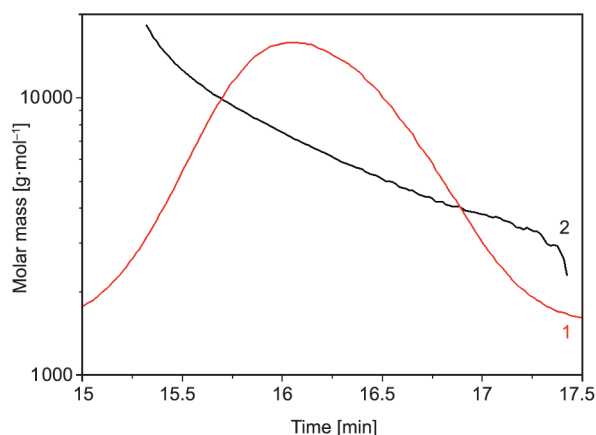


Figure 2. Graph of the molecular mass distribution (curve 1) and the Mark-Houwink plot (curve 2) of the PLGA-PEG-PLGA copolymer.

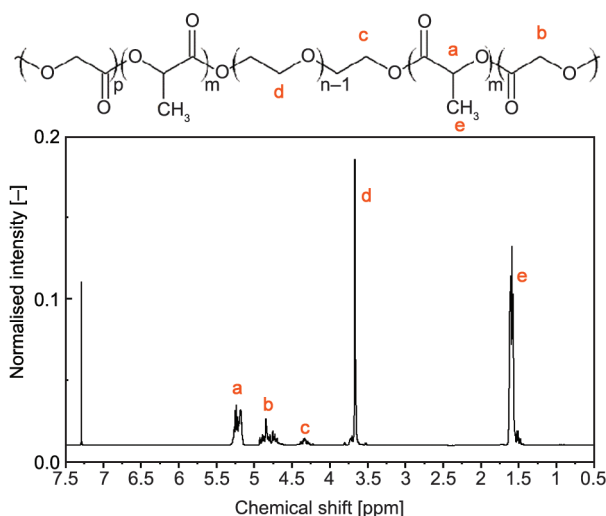


Figure 3. ^1H NMR spectrum of PLGA-PEG-PLGA triblock copolymer.

The rheological analysis was used to characterize the viscoelastic behavior depending on temperature (n . 5). From Figure 4 it is clear the PLGA-PEG-PLGA hydrogel undergoes two transitions characterized by two intersections of curves representing storage and loss modulus Figure 4. The first transition (sol-gel) is defined by an intersection at 33.5°C . The polymer increases its storage modulus, and due to the amphiphilic

Table 2. PLGA-PEG-PLGA polymer characterization.

		Theoretical and literature values of PLGA-PEG-PLGA	Measured values of PLGA-PEG-PLGA
M_n [$\text{g}\cdot\text{mol}^{-1}$]	GPC	5250	5600 ± 120
	^1H NMR		5300
PDI		1.100	1.11 ± 0.01
PLGA/PEG	[wt./wt.]	2.50	2.60
LA/GA	[mol/mol]	3.00	2.95
Temperature gel range 15 wt% [$^\circ\text{C}$]		$\approx 33.0\text{--}43.0$ [36, 37]	$33.5\text{--}41.8$

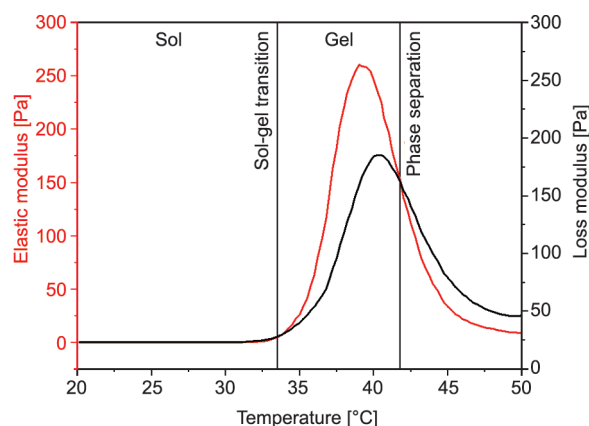


Figure 4. Temperature ramp and sol-gel area of 15 wt% PLGA-PEG-PLGA/albumin.

character of PLGA-PEG-PLGA, the organizing of polymeric chains to flower-like micelles forming hydrogel begins. After the storage modulus reaches its maximum, rapid decline occurs, followed by the second transition at 41.8 °C when the gel structure begins to collapse due to the micelle's dehydration leading to phase separation. Since albumin is the largest protein used in this study, it was intentionally added into the hydrogel for the purpose of this characterization to find whether the protein addition can affect the sol-gel transition. Compared with PLGA-PEG-PLGA hydrogel, no significant influence was observed. The temperature range at which the PLGA-PEG-PLGA/albumin is a gel is stated in Table 2.

3.2. Degradation of the PLGA-PEG-PLGA hydrogel scaffold

PLGA-PEG-PLGA hydrogel dissolved in PBS gradually lost its weight Figure 5 (n. 10). The hydrogel lost about 6% of its weight after 3 days. Significant mass loss occurred after 16 days (weight loss 31.4%),

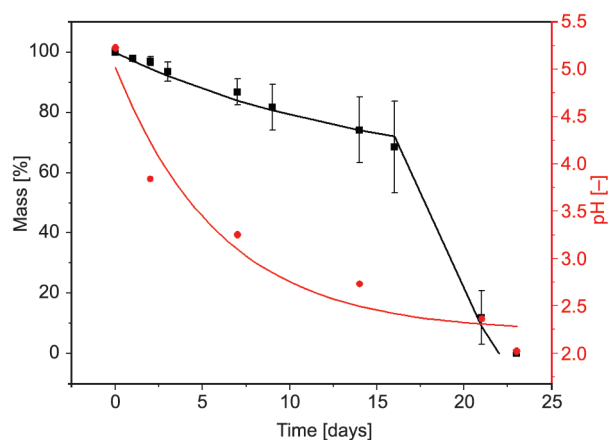


Figure 5. Weight loss and pH changes of 15 wt% PLGA-PEG-PLGA hydrogel scaffold in PBS solution in time.

and the hydrogel was completely decomposed after 23 days. The pH of the hydrogel scaffold was another important parameter that can affect the degradation, release rate, and activity of the incorporated protein. The pH of 15 wt% hydrogel after dissolution in PBS and incubation at 37 °C was 5.2 at day 0. pH decreased over time from 5.2 to 2.3 (see Figure 5).

3.3. Release of model proteins (albumin, lysozyme) from PLGA-PEG-PLGA hydrogel scaffolds

Two proteins were selected, namely human lysozyme, and human albumin for model release from 15 wt% PLGA-PEG-PLGA hydrogel scaffold. Lysozyme has a lower molecular weight ($14.7 \text{ kg} \cdot \text{mol}^{-1}$ [38]), and albumin is larger ($66.5 \text{ kg} \cdot \text{mol}^{-1}$ [39]) than FGF2-STAB[®] ($19 \text{ kg} \cdot \text{mol}^{-1}$). The measurements lasted 28 days, samples were taken at 1, 2, 3, 7, 9, 14, 16, 21, 23, and 28 days at 37 °C in an incubator, and the two-step release of proteins was monitored. For both the lysozyme and albumin, rapid release was observed (see Figure 6), approximately one-third of the incorporated proteins were released in 3 days. In the period 3 to 16 days, there was no measured release of proteins. The second release step was recorded from approximately 16 days of measurement, and after 28 days, 90% of the lysozyme and 70% of the albumin were released (n. 7).

3.4. FGF2-STAB[®] release from PLGA-PEG-PLGA hydrogel carrier

The treatment promoting growth factor release model was studied. Samples were first measured cumulatively with a set of samples (dynamic method, n. 7). The PBS solution into which the protein was released

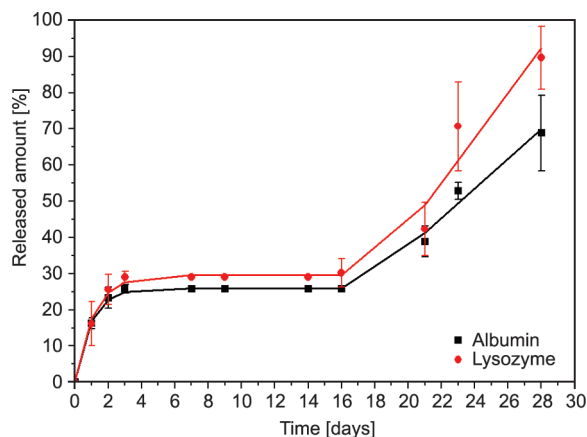


Figure 6. Albumin and lysozyme release from 15 wt% thermosensitive PLGA-PEG-PLGA hydrogel.

was changed after each collection (samples were taken at 1, 2, 3, 7, 9, 14, 16 and 21 days). In the second method (static method, n. 3) a sample was prepared for each collection separately, and a PBS solution was not changed (measurements after 1, 2, 3, 7, and 14 days). FGF2-STAB[®] release measurement using the static method was shorter than the dynamic method caused by faster sample degradation due to the lower pH of the immersed solution. UV-VIS spectrophotometry (Biochrom Libra S22) and SDS-PAGE electrophoresis were used for protein quantification. The pH of the immersed solution was also monitored. One-step protein release was observed. Figure 7 shows the initial burst release lasted on the third day (corresponding to approximately 50% of protein release). Then a slight slowdown was evident, and on the seventh day, a faster increase was observed. In general, during the measurement, 90% of the protein was released after 21 days. In case PBS solution was changed at each sampling, the pH has not dramatically dropped and ranged

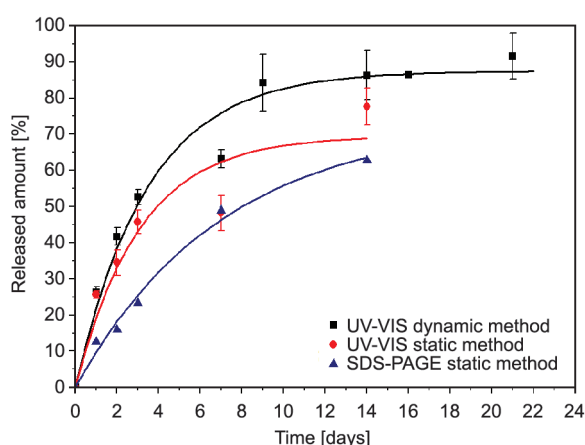


Figure 7. The amount of FGF2-STAB[®] released from 15 wt% PLGA-PEG-PLGA hydrogel in PBS.

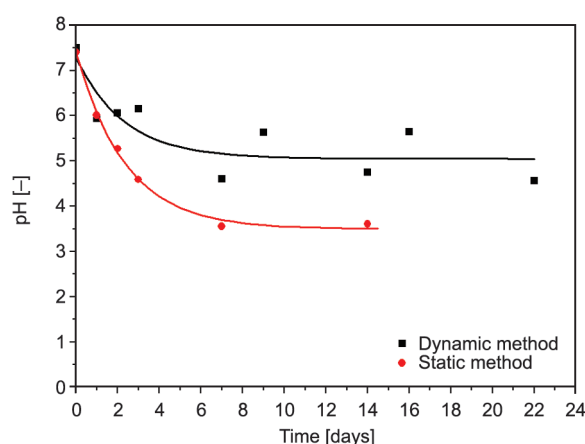


Figure 8. The pH of the immersed solutions, both for dynamic method and static method.

between 7–5 (see Figure 8). In a second way, when the PBS solution was not changed, the pH dropped to 3.6 after 14 days.

3.5. Proteins release kinetic study

The release regression was performed by a combination of three types of models:

1. The Higuchi model assumes that the release is controlled by Fickian diffusion. The model describes the concentration of the released compound as a function of the square root of time $Q = kt^{1/2}$, where k is the rate constant.
2. The zero-order kinetics assumes that the release is a consequence of carrier degradation. It is a linear function of time ($Q = kt$).
3. The first-order kinetics follows the effect when the concentration of compound in the carrier gradually decreases during release. It leads to exponential growth: $Q = A[1 - \exp(-kt)]$ where A is a limit concentration released from the carrier and k is the rate constant [40].

The assumed model was that in the first phase substances were released from the surface of the micelles. The first process was analyzed by the model. The models were compared using the R -square coefficient. For albumin, the zero-order kinetic model: $R^2 = 0.819$, Higuchi model: $R^2 = 0.903$; and the first-order kinetics: $R^2 = 0.9941$. Similar relations were also observed for the lysozyme (0.862, 0.919 and 0.976) and FGF2-STAB[®] (0.768, 0.937, and 0.983). Based on the value of R^2 , the optimal was first-order kinetics.

The process was analyzed using a function with the following condition (Equation (1) and (2)):

$$\begin{cases} t \leq t_{\text{delay}}; & Q = A[1 - e^{-k_1 t}] \\ t > t_{\text{delay}}; & Q = A[1 - e^{-k_1 t}] + k_2(t - t_{\text{delay}}) \end{cases} \quad (1)$$

$$(2)$$

where Q was released amount of the active compounds, delay of micelles decomposition t_{delay} was a variable parameter obtained from the regression. The rate constant k_1 was transformed into the half-time of release a time when half of the maximal capacity was released in the first step (Equation (3)):

$$t_{1/2} = \frac{\ln 2}{k_1} \quad (3)$$

The regression constant k_2 was recalculated. In the case that the active compound did not participate in the kinetic process, the rate constant includes

information on the concentration of the active compounds (Equation (4)):

$$k_2 = k_{\text{eff}}[AC] \quad (4)$$

where $[AC]$ was the concentration of the active compound and k_{eff} was the effective rate constant of the micellar decomposition the effective rate constant enables us to compare the rate of micellar decomposition in different cases. Table 3 shows all parameters obtained by regression analysis.

The regression analysis was applied to the gel degradation. The gel was degraded in two steps, and the second step was observed with a certain delay. The first phase started immediately after swelling, and it degraded 41% of the gel. The half-time of the first phase was 9.7 days. The first active compound was significantly faster - the half-time was from 0.65 to 2.4 days. The second phase of degradation started with a delay of 17.8 days, which was in accordance with the delay of the second phase of release. The degradation phase was significantly faster than the release phase. The half-time of decomposition was 0.2 days, which meant that the gel structure was destroyed very quickly after the delay period. However, the release was observed even several days after

the delay period. It was probable that the gel structure was destroyed, but active compounds were still present in isolated micelles.

3.6. *In vitro* biological activity of FGF2-STAB®

The biological activity of FGF2-STAB® released from the PLGA-PEG-PLGA hydrogel matrix was verified by proliferation assay using BaF3-FGFR2c cells. FGF2-STAB® extracts were prepared in time intervals 0, 1, 2, 3, 7, and 14 days (static method) and after 7 and 14 days (dynamic method) of protein release from the hydrogel. For each time point, a protein sample extract was prepared. All tested FGF2-STAB® samples effectively induced proliferation of BaF3-FGFR2c cells, and all samples reached almost the same maximal response. Comparison of the half-maximal effective dose (ED_{50}) revealed that FGF2-STAB® released from the hydrogel in time intervals 1–7 days (static method) exhibited comparable activity as the free protein ($ED_{50} < 1.0 \text{ ng} \cdot \text{mL}^{-1}$). The only effect on the protein activity was detected for FGF2-STAB® sample released from the hydrogel after 14 days, where a one-order of magnitude drop in ED_{50} value was detected ($ED_{50} = 4.4 \text{ ng} \cdot \text{mL}^{-1}$) (Figure 9a). On the other hand, in the dynamic method, the protein showed unmodified activity even after 14 days (Figure 9b).

Table 3. Parameters obtained from regression.

Parameter	Symbolum	Unit	Albumin	Lysosome	FGF2-STAB®
Saturation capacity of micellar surface	A	[%]	26.0	29.6	87.5
Rate constant	k_1	[day ⁻¹]	1.05	0.90	0.29
Half-time of the release	$t_{1/2}$	[days]	0.658	0.770	2.400
Rate constant from regression	k_2	[day ⁻¹]	4.076	6.194	1.027
Effective rate constant of micellar decomposition	k_{eff}	[day ⁻¹]	0.055	0.088	0.082*
Delay of the degradation	t_0	[days]	17.2	17.9	17.0*

*estimation from two experimental points.

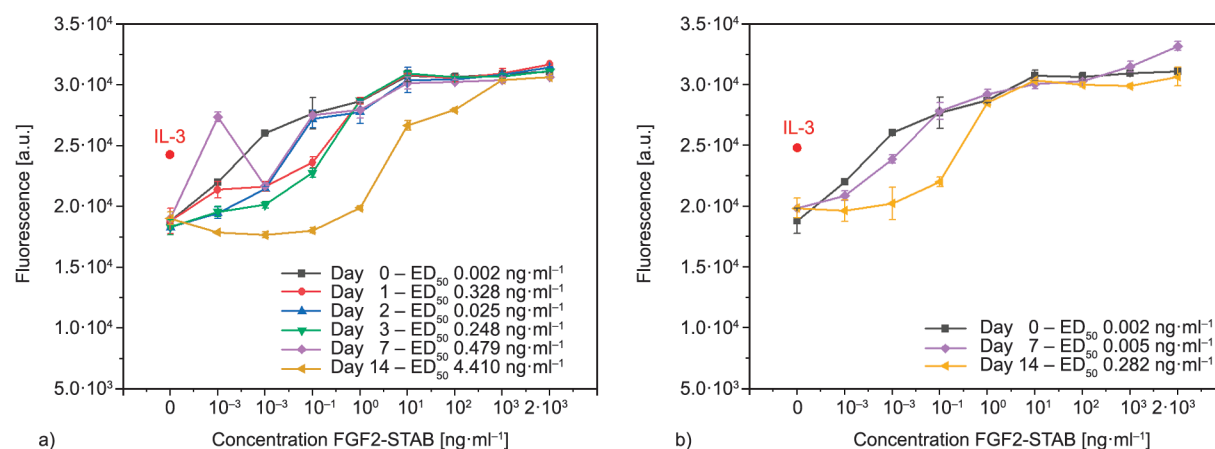


Figure 9. Biological activity of FGF2-STAB® samples released from the PLGA-PEG-PLGA hydrogel. a) Static method, b) dynamic method.

4. Discussion

PLGA-PEG-PLGA hydrogels [36] have great advantages over other drug delivery materials (PNIPAAm [41], pluronic® [42] – discussed toxicity of degradation products, chitosan [43] – poor solubility, and polyethylene glycol/polycaprolactone – PEG/PCL [44] – problem with high crystallinity and hydrophobicity of PCL) for application in reconstructive medicine in combination with proteins promoted healing [45, 46]. It is biodegradable, biocompatible, and stable over 16 days. However, the degradation time, as well as the polarity or gelation temperature [37], can be adjusted by the LA/GA and PLGA/PEG ratios for specific application [22–24, 47]. The PLGA-PEG-PLGA hydrogel is also soluble in water, and there is no need to use organic solvents [8]. Hydrogel can be injected directly into the body when it forms a gel at human body temperature [6, 24, 48, 49]. Moreover, due to the thixotropic character of PLGA-PEG-PLGA solution, there is no risk of leakage into the surrounding tissue, and it stays at the site of administration [15, 43, 50]. The use of inserts was also innovative, as there was no direct manipulation of the sample during PBS solution collection (see Figure 1). Thus, it was not possible to damage samples, as in the case of a conventional re-coating of the hydrogel with a solution and subsequent sampling [51–54]. Cost-effective albumin and lysozyme were chosen for model release from thermosensitive PLGA-PEG-PLGA hydrogel. Two-step proteins release (see Figure 6) was observed. From the kinetic models was assumed that the bioactive compound (lysozyme, albumin) was located partly on the surface of the micelle and partly inside the micelle. The compound

was released from the surface of the micelles in the first step. At the same time, the concentration of adsorbed compounds decreases, which was why the best model for the first step was first-order kinetics. Subsequently, the decomposition of micelles from the second step was observed with a certain delay after the first step of release. The degradation in the second step was analyzed by zero-order kinetics because it was supposed that the active compound did not interfere with the degradation process (Figure 10) [40, 51]. The difference between the amount of albumin and the lysozyme released was due to the distinction in the molecular weights of the proteins and mainly the polarity rate. Since both proteins had polar and non-polar residues on the surface of the molecule, it was differently bound to the hydrogel micelles [55]. There are more polar groups on the surface of lysozyme, therefore, more protein was probably bound to the micelle surface, and only part of it was in its center. Thus, a higher total amount of lysozyme protein was released [56]. On the contrary, albumin on the surface was more non-polar, it had 11 hydrophobic binding sites and was thus more bound to the center of the micelle while only a portion remained on the surface [57]. This resulted in a lower release efficiency comparing the lysozyme. The second step occurred at a time when the PLGA-PEG-PLGA hydrogel was gradually degraded, and proteins bound to the micelle center were released. Yu *et al.* [45] proved one-step lysozyme release from PLGA-PEG-PLGA hydrogel. This supports the hypothesis that triblock copolymer influences the composition (*e.g.*, LA/GA ratios etc.) of the protein release mechanism.

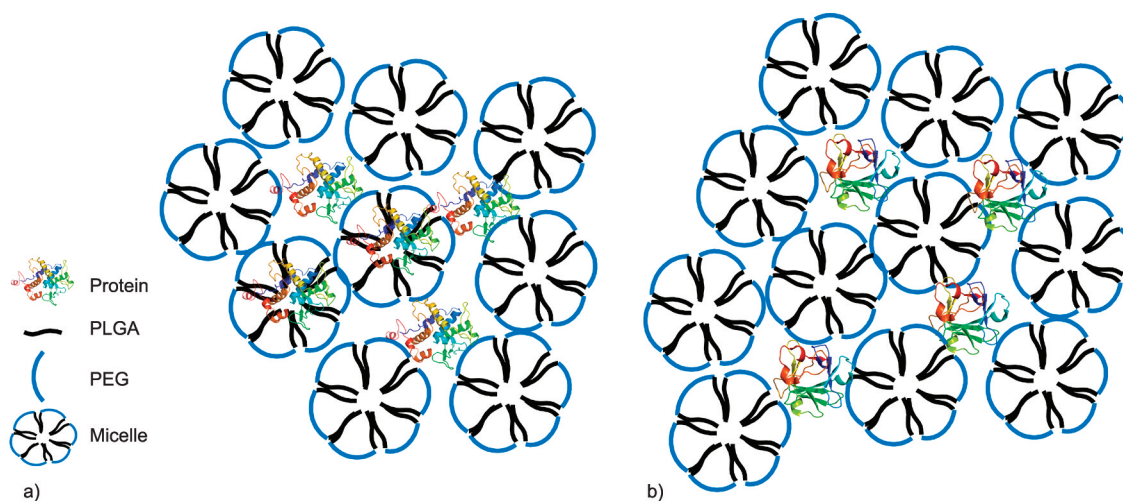


Figure 10. Protein incorporation scheme a) lysozyme, albumin; b) FGF2-STAB® into micellar structure of the hydrogel scaffold.

Stable fibroblast growth factor 2 (FGF2-STAB[®] – 19 kg·mol⁻¹, provided by Enantis Ltd. [27, 28]) was chosen as a bioactive substance because it promotes healing and leads to tissue remodeling [26]. Since FGF2-STAB[®] is hydrophilic due to the presence of Arg, Cys, and Ser residues on the protein surface, most of the FGF2-STAB[®] was bound to the micelle shell present in the hydrogel (see Figure 10) [26]. This was proved by kinetic models, which confirmed first-order kinetics controlled mainly by decreasing the concentration of the active compound in the matrix and, at a later stage, by minor matrix degradation [58, 59]. The initial release was diffusion-dependent [60], and most FGF2-STAB[®] was released from the hydrogel carrier over the first three days. After 16 days, the hydrogel began to degrade more rapidly, leading to a consequently increased release of protein [55, 61]. The degradation of 15 wt% of the hydrogel occurred gradually (see Figure 5) [24]. The increase in weight loss over time was also caused by the formation of acid degradation products (lactide acid and glycolide acid), which accelerated the degradation [35, 62]. Samples, measured by the static method, were monitored for only 14 days due to faster degradation of the hydrogel matrix. As there was no change in the solution into which the proteins were released, there was faster acidification and formation of degradation products. Overall, the degradation of the hydrogel matrix was set at approximately 20–23 days, which is the half-life of FGF2-STAB[®] [28], and approximately 90% of the protein was released at that time. In contrast to other studies where the degradation of the scaffold and the release of drugs and proteins were set at up to 30–60 days [45, 51, 53, 54, 63].

The formation of acidic products could also affect the pH of the immersed solution, which could lead to a loss of protein activity [43]. *in vitro* biological activity of the protein was verified by proliferation assay using the BaF3 model system. For samples in which the PBS was changed after each collection (dynamic method), observation indicates that the protein functionality is not affected either by the incorporation into the PLGA-PEG-PLGA hydrogel matrix or by its release from the hydrogel in time intervals up to 14 days. In the static method, the protein activity drop was observed that could be attributed to the low pH (pH 3.6) of protein extract, probably connected with gradual hydrogel degradation to acidic degradation products. On the other hand, the human body

is a sophisticated dynamic system that allows waste products to be processed, so it is assumed there is no risk of concentration of polymer degradation products. Hence, the protein activity need not be compromised by low pH. Moreover, the PLGA-PEG-PLGA degrades to lactic acid, glycolic acid, and polyethylene glycol, which can be metabolised to CO₂ and water via Krebs cycle [32].

5. Conclusions

In this study, protein release from the thermosensitive injectable PLGA-PEG-PLGA hydrogel was monitored. The PLGA-PEG-PLGA hydrogel scaffold has proven to be a suitable carrier for stable fibroblast growth factor 2 (FGF2-STAB[®]). FGF2-STAB[®] (produced by Enantis company, stable at 37 °C for up to 20 days) in combination with injectable thermosensitive PLGA-PEG-PLGA hydrogel scaffold provides a promising protein-delivery system for further use in regenerative medicine. The protein was gradually released over 21 days, which is suitable for use in regenerative medicine. First-order kinetics were controlled mainly by decreasing concentrations of active compounds in the matrix and, at a later stage, by matrix degradation. Although the pH of the hydrogel and the immersed extract dropped below 6, there was no loss of biological activity of the stabilized released protein. The combination of the PLGA-PEG-PLGA hydrogel and FGF2-STAB[®] appears promising for further use and will be the subject of another research.

Acknowledgements

Grant Low temperature 3D printed bioresorbable hydrogels as carriers of pro-healing protein for tissue regeneration is realized within the project Quality Internal Grants of BUT (KInG BUT), Reg. No. CZ.02.2.69 / 0.0 / 0.0 / 19_073 / 0016948, which is financed from the OP RDE.

Authors greatly appreciate the collaboration with Enantis, Ltd., which provided the stabilized protein FGF2-STAB[®] for this project. All rights reserved. We thank doc. MUDr. Břetislav Lipový, PhD., MBA for application consultation and dr. Pawel Jewula from CEITEC BUT for NMR measurement at Dadok's NMR Centrum at Masaryk University.

References

- [1] Chhibber T., Shinde R., Lahooti B., Bagchi S., Varahachalam S. P., Gaddam A., Jaiswal A. K., Gracia E., Chand H. S., Kaushik A., Jayant R. D.: Hydrogels in tissue engineering. in 'Intelligent hydrogels in diagnostics and therapeutics' CRC Press, Boca Raton, 105–122 (2020).

- [2] Shafer K. E., Cohen A. C., Wiebke E. A.: Novel approach to surgical repair of enterovaginal fistula in the irradiated pelvis. *Plastic and Reconstructive Surgery*, **130**, 385e–386e (2012).
<https://doi.org/10.1097/PRS.0b013e3182590374>
- [3] Lee G., Hunter-Smith D. J., Rozen W. M.: Autologous fat grafting in keloids and hypertrophic scars: A review. *Scars, Burns and Healing*, **3**, 1–6 (2017).
<https://doi.org/10.1177/2059513117700157>
- [4] Kenny E. M., Egro F. M., Ejaz A., Coleman S. R., Greenberger J. S., Rubin J. P.: Fat grafting in radiation-induced soft-tissue injury: A narrative review of the clinical evidence and implications for future studies. *Plastic and Reconstructive Surgery*, **147**, 819–838 (2021).
<https://doi.org/10.1097/PRS.00000000000007705>
- [5] Choi M., Small K., Levovitz C., Lee C., Fadl A., Karp N. S.: The volumetric analysis of fat graft survival in breast reconstruction. *Plastic and Reconstructive Surgery*, **131**, 185–191 (2013).
<https://doi.org/10.1097/PRS.0b013e3182789b13>
- [6] Chamradová I., Vojtová L., Michlovská L., Poláček P., Jančář J.: Rheological properties of functionalised thermosensitive copolymers for injectable applications in medicine. *Chemical Papers*, **66**, 977–980 (2012).
<https://doi.org/10.2478/s11696-012-0210-y>
- [7] Priya James H., John R., Alex A., Anoop K. R.: Smart polymers for the controlled delivery of drugs – A concise overview. *Acta Pharmaceutica Sinica B*, **4**, 120–127 (2014).
<https://doi.org/10.1016/j.apsb.2014.02.005>
- [8] Gao Y., Ren F., Ding B., Sun N., Liu X., Ding X., Gao S.: A thermo-sensitive PLGA-PEG-PLGA hydrogel for sustained release of docetaxel. *Journal of Drug Targeting*, **19**, 516–527 (2011).
<https://doi.org/10.3109/1061186X.2010.519031>
- [9] Jeong B., Bae Y. H., Kim S. W.: Drug release from biodegradable injectable thermosensitive hydrogel of PEG-PLGA-PEG triblock copolymers. *Journal of Controlled Release*, **63**, 155–163 (2000).
[https://doi.org/10.1016/S0168-3659\(99\)00194-7](https://doi.org/10.1016/S0168-3659(99)00194-7)
- [10] Gervais K. J.: Evaluation of a biodegradable thermogel polymer for intraocular delivery of cyclosporine A to prevent posterior capsule opacification. Thesis, Ohio State University (2017).
- [11] Desai K. G. H., Olsen K. F., Mallery S. R., Stoner G. D., Schwendeman S. P.: Formulation and *in vitro-in vivo* evaluation of black raspberry extract-loaded PLGA/PLA injectable millicylindrical implants for sustained delivery of chemopreventive anthocyanins. *Pharmaceutical Research*, **27**, 628–643 (2010).
<https://doi.org/10.1007/s11095-009-0038-5>
- [12] Liechty W. B., Kryscio D. R., Slaughter B. V., Peppas N. A.: Polymers for drug delivery systems. *Annual Review of Chemical and Biomolecular Engineering*, **1**, 149–173 (2010).
<https://doi.org/10.1146/annurev-chembioeng-073009-100847>
- [13] Jusu S. M., Obayemi J. D., Salifu A. A., Nwazojie C. C., Uzonwanne V., Odusanya O. S., Soboyejo W. O.: Drug-encapsulated blend of PLGA-PEG microspheres: *In vitro* and *in vivo* study of the effects of localized/targeted drug delivery on the treatment of triple-negative breast cancer. *Scientific Reports*, **10**, 14188 (2020).
<https://doi.org/10.1038/s41598-020-71129-0>
- [14] Elstad N. L., Fowers K. D.: OncoGel (ReGel/paclitaxel) – Clinical applications for a novel paclitaxel delivery system. *Advanced Drug Delivery Reviews*, **61**, 785–794 (2009).
<https://doi.org/10.1016/j.addr.2009.04.010>
- [15] Zahoranova A., Vojtova L., Dusicka E., Michlovská L., Krivankova N., Baudis S.: Hybrid hydrogel networks by photocrosslinking of thermoresponsive α,ω -itaconyl-PLGA-PEG-PLGA micelles in water: Influence of the lithium phenyl-2,4,6-trimethylbenzoylphosphine photoinitiator. *Macromolecular Chemistry and Physics*, **221**, 2000165 (2020).
<https://doi.org/10.1002/macp.202000165>
- [16] Perinelli D. R., Cespi M., Bonacucina G., Palmieri G. F.: PEGylated polylactide (PLA) and poly (lactic-co-glycolic acid) (PLGA) copolymers for the design of drug delivery systems. *Journal of Pharmaceutical Investigation*, **49**, 443–458 (2019).
<https://doi.org/10.1007/s40005-019-00442-2>
- [17] Jain A., Kunduru K. R., Basu A., Mizrahi B., Domb A. J., Khan W.: Injectable formulations of poly(lactic acid) and its copolymers in clinical use. *Advanced Drug Delivery Reviews*, **107**, 213–227 (2016).
<https://doi.org/10.1016/j.addr.2016.07.002>
- [18] Osorno L. L., Maldonado D. E., Whitener R. J., Brandley A. N., Yiantos A., Medina J. D. R., Byrne M. E.: Amphiphilic PLGA-PEG-PLGA triblock copolymer nanogels varying in gelation temperature and modulus for the extended and controlled release of hyaluronic acid. *Journal of Applied Polymer Science*, **137**, 48678 (2020).
<https://doi.org/10.1002/app.48678>
- [19] Kitagawa M., Maeda T., Hotta A.: PEG-based nanocomposite hydrogel: Thermo-responsive sol-gel transition and degradation behavior controlled by the LA/GA ratio of PLGA-PEG-PLGA. *Polymer Degradation and Stability*, **147**, 222–228 (2018).
<https://doi.org/10.1016/j.polymdegradstab.2017.11.024>
- [20] Jain R. A.: The manufacturing techniques of various drug loaded biodegradable poly(lactide-co-glycolide) (PLGA) devices. *Biomaterials*, **21**, 2475–2490 (2000).
[https://doi.org/10.1016/S0142-9612\(00\)00115-0](https://doi.org/10.1016/S0142-9612(00)00115-0)
- [21] Su C., Liu Y., Li R., Wu W., Fawcett J. P., Gu J.: Absorption, distribution, metabolism and excretion of the biomaterials used in nanocarrier drug delivery systems. *Advanced Drug Delivery Reviews*, **143**, 97–114 (2019).
<https://doi.org/10.1016/j.addr.2019.06.008>
- [22] Makadia H. K., Siegel S. J.: Poly lactic-co-glycolic acid (PLGA) as biodegradable controlled drug delivery carrier. *Polymers*, **3**, 1377–1397 (2011).
<https://doi.org/10.3390/polym3031377>

- [23] Chung H. J., Park T. G.: Self-assembled and nanostructured hydrogels for drug delivery and tissue engineering. *Nano Today*, **4**, 429–437 (2009).
<https://doi.org/10.1016/j.nantod.2009.08.008>
- [24] Oborná J., Mravcová L., Michlovská L., Vojtová L., Vávrová M.: The effect of PLGA-PEG-PLGA modification on the sol-gel transition and degradation properties. *Express Polymer Letters*, **10**, 361–372 (2016).
<https://doi.org/10.3144/expresspolymlett.2016.34>
- [25] Chen Y., Shi J., Zhang Y., Miao J., Zhao Z., Jin X., Liu L., Yu L., Shen C., Ding J.: An injectable thermosensitive hydrogel loaded with an ancient natural drug colchicine for myocardial repair after infarction. *Journal of Materials Chemistry B*, **8**, 980–992 (2020).
<https://doi.org/10.1039/C9TB02523E>
- [26] Nugent M. A., Iozzo R. V.: Fibroblast growth factor-2. *The International Journal of Biochemistry and Cell Biology*, **32**, 115–120 (2000).
[https://doi.org/10.1016/S1357-2725\(99\)00123-5](https://doi.org/10.1016/S1357-2725(99)00123-5)
- [27] Dvorak P., Krejci P., Balek L., Eiselleova L., Konecna Z., Dvorak P., Bednar D., Brezovsky J., Sebestova E., Chaloupkova R., Stepankova V., Vanacek P., Prokop Z., Damborsky J., Bosakova M.: Thermostable FGF2 polypeptide, use thereof. EP 3380508 B1, Czech Republic (2018).
- [28] Dvorak P., Bednar D., Vanacek P., Balek L., Eiselleova L., Stepankova V., Sebestova E., Kunova Bosakova M., Konecna Z., Mazurenko S., Kunka A., Vanova T., Zoufalova K., Chaloupkova R., Brezovsky J., Krejci P., Prokop Z., Dvorak P., Damborsky J.: Computer-assisted engineering of hyperstable fibroblast growth factor 2. *Biotechnology and Bioengineering*, **115**, 850–862 (2018).
<https://doi.org/10.1002/bit.26531>
- [29] Muchová J., Hearnden V., Michlovská L., Vištejnová L., Zavaďáková A., Šmerková K., Kočiová S., Adam V., Kopel P., Vojtová L.: Mutual influence of selenium nanoparticles and FGF2-STAB[®] on biocompatible properties of collagen/chitosan 3D scaffolds: *In vitro* and *ex ovo* evaluation. *Journal of Nanobiotechnology*, **19**, 103 (2021).
<https://doi.org/10.1186/s12951-021-00849-w>
- [30] Vojtová L., Pavliňáková V., Muchová J., Kacvinská K., Brtníková J., Knoz M., Lipový B., Faldyna M., Göpfert E., Holoubek J., Pavlovský Z., Vícenová M., Blahnová V. H., Hearnden V., Filová E.: Healing and angiogenic properties of collagen/chitosan scaffolds enriched with hyperstable FGF2-STAB[®] protein: *In vitro*, *ex ovo* and *in vivo* comprehensive evaluation. *Biomedicines*, **9**, 590 (2021).
<https://doi.org/10.3390/biomedicines9060590>
- [31] Krticka M., Planka L., Vojtova L., Nekuda V., Stastny P., Sedlacek R., Brinek A., Kavkova M., Gopfert E., Hedvicakova V., Rampichova M., Kren L., Liskova K., Ira D., Dorazilová J., Suchy T., Zikmund T., Kaiser J., Stary D., Faldyna M., Trunec M.: Lumbar interbody fusion conducted on a porcine model with a bioresorbable ceramic/biopolymer hybrid implant enriched with hyperstable fibroblast growth factor 2. *Biomedicines*, **9**, 733 (2021).
<https://doi.org/10.3390/biomedicines9070733>
- [32] Michlovská L., Vojtová L., Mravcová L., Hermanová S., Kučerík J., Jančář J.: Functionalization conditions of PLGA-PEG-PLGA copolymer with itaconic anhydride. *Macromolecular Symposia*, **295**, 119–124 (2010).
<https://doi.org/10.1002/masy.200900071>
- [33] Bárta J., Bártová V., Čurn V.: Protein analysis using automated experion chip electrophoresis and its comparison with SDS-PAGE (in Czech). *Chemicke Listy*, **104**, 33–40 (2010).
- [34] Ornitz D. M., Xu J., Colvin J. S., McEwen D. G., MacArthur C. A., Coulier F., Gao G., Goldfarb M.: Receptor specificity of the fibroblast growth factor family. *Journal of Biological Chemistry*, **271**, 15292–15297 (1996).
<https://doi.org/10.1074/jbc.271.25.15292>
- [35] Michlovská L., Vojtová L., Humpa O., Kučerík J., Židek J., Jančář J.: Hydrolytic stability of end-linked hydrogels from PLGA–PEG–PLGA macromonomers terminated by α,ω -itaconyl groups. *RSC Advances*, **6**, 16808–16816 (2016).
<https://doi.org/10.1039/C5RA26222D>
- [36] Vojtova L., Michlovska L., Valova K., Zboncak M., Trunec M., Castkova K., Krticka M., Pavlinakova V., Polacek P., Dzurov M., Lukasova V., Rampichova M., Suchy T., Sedlacek R., Ginebra M-P., Montufar E.: The effect of the thermosensitive biodegradable PLGA–PEG–PLGA copolymer on the rheological, structural and mechanical properties of thixotropic self-hardening tricalcium phosphate cement. *International Journal of Molecular Sciences*, **20**, 391 (2019).
<https://doi.org/10.3390/ijms20020391>
- [37] Cespi M., Bonacucina G., Tiboni M., Casettari L., Cambriani A., Fini F., Perinelli D. R., Palmieri G. F.: Insights in the rheological properties of PLGA-PEG-PLGA aqueous dispersions: Structural properties and temperature-dependent behaviour. *Polymer*, **213**, 123216 (2021).
<https://doi.org/10.1016/j.polymer.2020.123216>
- [38] Wu H., Cao D., Liu T., Zhao J., Hu X., Li N.: Purification and characterization of recombinant human lysozyme from eggs of transgenic chickens. *PLoS ONE*, **10**, e0146032 (2015).
<https://doi.org/10.1371/journal.pone.0146032>

- [39] Pappa T., Refetoff S.: Thyroid hormone transport proteins: Thyroxine-binding globulin, transthyretin, and albumin. in 'Reference module in neuroscience and behavioral psychology' Elsevier, Amsterdam, 483–490 (2017).
<https://doi.org/10.1016/B978-0-12-809324-5.03494-5>
- [40] Paarakh M. P., Jose P. A. N. I., Setty C. M., Peter G. V.: Release kinetic – concepts and applications. International Journal of Pharmacy Research and Technology, **8**, 12–20 (2019).
- [41] Cooperstein M. A., Canavan H. E.: Assessment of cytotoxicity of (*N*-isopropyl acrylamide) and poly(*N*-isopropyl acrylamide)-coated surfaces. Biointerphases, **8**, 19 (2013).
<https://doi.org/10.1186/1559-4106-8-19>
- [42] Wang R., Hughes T., Beck S., Vakil S., Li S., Pantano P., Draper R. K.: Generation of toxic degradation products by sonication of Pluronic® dispersants: Implications for nanotoxicity testing. Nanotoxicology, **7**, 1272–1281 (2012).
<https://doi.org/10.3109/17435390.2012.736547>
- [43] Talley K., Alexov E.: On the pH-optimum of activity and stability of proteins. Proteins: Structure, Function, and Bioinformatics, **78**, 2699–2706 (2010).
<https://doi.org/10.1002/prot.22786>
- [44] Deng H., Dong A., Song J., Chen X.: Injectable thermosensitive hydrogel systems based on functional PEG/PCL block polymer for local drug delivery. Journal of Controlled Release, **297**, 60–70 (2019).
<https://doi.org/10.1016/j.jconrel.2019.01.026>
- [45] Yu L., Zhang Z., Zhang H., Ding J.: Mixing a sol and a precipitate of block copolymers with different block ratios leads to an injectable hydrogel. Biomacromolecules, **10**, 1547–1553 (2009).
<https://doi.org/10.1021/bm900145g>
- [46] White L. J., Kirby G. T. S., Cox H. C., Qodratnama R., Qutachi O., Rose F. R. A. J., Shakesheff K. M.: Accelerating protein release from microparticles for regenerative medicine applications. Materials Science and Engineering: C, **33**, 2578–2583 (2013).
<https://doi.org/10.1016/j.msec.2013.02.020>
- [47] Qiao M., Chen D., Ma X., Liu Y.: Injectable biodegradable temperature-responsive PLGA-PEG-PLGA copolymers: Synthesis and effect of copolymer composition on the drug release from the copolymer-based hydrogels. International Journal of Pharmaceutics, **294**, 103–112 (2005).
<https://doi.org/10.1016/j.ijpharm.2005.01.017>
- [48] Narayanaswamy R., Torchilin V. P.: Hydrogels and their applications in targeted drug delivery. Molecules, **24**, 603 (2019).
<https://doi.org/10.3390/molecules24030603>
- [49] Zhang L., Shen W., Luan J., Yang D., Wei G., Yu L., Lu W., Ding J.: Sustained intravitreal delivery of dexamethasone using an injectable and biodegradable thermogel. Acta Biomaterialia, **23**, 271–281 (2015).
<https://doi.org/10.1016/j.actbio.2015.05.005>
- [50] Gong Z., Yang Y., Ren Q., Chen X., Shao Z.: Injectable thixotropic hydrogel comprising regenerated silk fibroin and hydroxypropylcellulose. Soft Matter, **8**, 2875–2883 (2012).
<https://doi.org/10.1039/c2sm06984a>
- [51] Kamali H., Khodaverdi E., Kaffash E., Saffari A. S., Shiadeh S. N. R., Nokhodchi A., Hadizadeh F.: Optimization and *in vitro* evaluation of injectable sustained-release of levothyroxine using PLGA-PEG-PLGA. Journal of Pharmaceutical Innovation, **16**, 688–698 (2021).
<https://doi.org/10.1007/s12247-020-09480-y>
- [52] Khodaverdi E., Tekie F. S. M., Mohajeri S. A., Ganji F., Zohuri G., Hadizadeh F.: Preparation and investigation of sustained drug delivery systems using an injectable, thermosensitive, *in situ* forming hydrogel composed of PLGA-PEG-PLGA. AAPS PharmSciTech, **13**, 590–600 (2012).
<https://doi.org/10.1208/s12249-012-9781-8>
- [53] Xie B., Jin L., Luo Z., Yu J., Shi S., Zhang Z., Shen M., Chen H., Li X., Song Z.: An injectable thermosensitive polymeric hydrogel for sustained release of Avastin® to treat posterior segment disease. International Journal of Pharmaceutics, **490**, 375–383 (2015).
<https://doi.org/10.1016/j.ijpharm.2015.05.071>
- [54] Qiao M., Chen D., Hao T., Zhao X., Hu H., Ma X.: Effect of bee venom peptide-copolymer interactions on thermosensitive hydrogel delivery systems. International Journal of Pharmaceutics, **345**, 116–124 (2007).
<https://doi.org/10.1016/j.ijpharm.2007.05.056>
- [55] Xu Y., Kim C.-S., Saylor D. M., Koo D.: Polymer degradation and drug delivery in PLGA-based drug-polymer applications: A review of experiments and theories. Journal of Biomedical Materials Research Part B: Applied Biomaterials, **105**, 1692–1716 (2017).
<https://doi.org/10.1002/jbm.b.33648>
- [56] Jafari M., Mehrnejad F.: Molecular insight into human lysozyme and its ability to form amyloid fibrils in high concentrations of sodium dodecyl sulfate: A view from molecular dynamics simulations. PLoS ONE, **11**, e0165213 (2016).
<https://doi.org/10.1371/journal.pone.0165213>
- [57] Retnaningtyas E., Sumitro S. B., Soeatmadji D. W., Widjayanto E.: Molecular dynamics simulation for revealing the role of water molecules on conformational change of human serum albumin. International Journal of Pharmaceutical and Clinical Research, **8**, 158–161 (2016).
<https://doi.org/10.25258/ijpcr.v8i3.1>
- [58] Fu Y., Kao W. J.: Drug release kinetics and transport mechanisms of non-degradable and degradable polymeric delivery systems. Expert Opinion on Drug Delivery, **7**, 429–444 (2010).
<https://doi.org/10.1517/17425241003602259>

- [59] Chen K., Chen X., Han X., Fu Y.: A comparison study on the release kinetics and mechanism of bovine serum albumin and nanoencapsulated albumin from hydrogel networks. *International Journal of Biological Macromolecules*, **163**, 1291–1300 (2020).
<https://doi.org/10.1016/j.ijbiomac.2020.07.043>
- [60] Pagels R. F., Prud'homme R. K.: Polymeric nanoparticles and microparticles for the delivery of peptides, biologics, and soluble therapeutics. *Journal of Controlled Release*, **219**, 519–535 (2015).
<https://doi.org/10.1016/j.jconrel.2015.09.001>
- [61] Kasyapi N., Dinesh Kumar K., Bhowmick A. K.: Influence of microstructure of lactone-based triblock copolymers on drug release behavior of their microspheres. *Journal of Applied Polymer Science*, **134**, 45284 (2017).
<https://doi.org/10.1002/app.45284>
- [62] Milacic V., Schwendeman S. P.: Lysozyme release and polymer erosion behavior of injectable implants prepared from PLGA-PEG block copolymers and PLGA/PLGA-PEG blends. *Pharmaceutical Research*, **31**, 436–448 (2014).
<https://doi.org/10.1007/s11095-013-1173-6>
- [63] Yang X., Trinh H. M., Agrahari V., Sheng Y., Pal D., Mitra A. K.: Nanoparticle-based topical ophthalmic gel formulation for sustained release of hydrocortisone butyrate. *AAPS PharmSciTech*, **17**, 294–306 (2016).
<https://doi.org/10.1208/s12249-015-0354-5>